AIP | Applied Physics Letters

Low symmetry phase in Pb (Zr 0.52 Ti 0.48) O 3 epitaxial thin films with enhanced ferroelectric properties

Li Yan, Jiefang Li, Hu Cao, and D. Viehland

Citation: Applied Physics Letters **89**, 262905 (2006); doi: 10.1063/1.2425016
View online: http://dx.doi.org/10.1063/1.2425016
View Table of Contents: http://scitation.aip.org/content/aip/journal/apl/89/26?ver=pdfcov
Published by the AIP Publishing

Low symmetry phase in $Pb(Zr_{0.52}Ti_{0.48})O_3$ epitaxial thin films with enhanced ferroelectric properties

Li Yan,[a] Jiefang Li, Hu Cao, and D. Viehland
Department of Materials Science and Engineering, Virginia Tech, Blacksburg, Virginia 24061

(Received 5 October 2006; accepted 25 November 2006; published online 28 December 2006)

The authors report the structural and ferroelectric properties of $Pb(Zr_{0.52}Ti_{0.48})O_3$ (PZT) epitaxial thin films grown on (001), (110), and (111) $SrRuO_3/SrTiO_3$ substrates by pulsed laser deposition. A monoclinic C (M_c) phase has been found for (101) films, whereas (001) and (111) ones were tetragonal (T) and rhombohedral (R), respectively. The authors find that the ferroelectric polarization of the M_c phase is higher than that in either the T or R ones. These results are consistent with predictions (i) of epitaxial phase diagrams and (ii) that the enhanced ferroelectric properties of morphotropic phase boundary PZT are related to a low symmetry monoclinic phase. © *2006 American Institute of Physics*. [DOI: 10.1063/1.2425016]

Lead zirconate titanate, $Pb(Zr_{1-x}Ti_x)O_3$ or PZT, is a ferroelectric perovskite widely used as piezoelectric actuators and sensors due to their superior piezoelectric coefficients. The phase diagram of $Pb(Zr_{1-x}Ti_x)O_3$ can be found in the work of Jaffe *et al.*[1] Outstanding piezoelectric properties occur in the vicinity of a morphotropic phase boundary (MPB) between tetragonal (T) and rhombohedral (R) ferroelectric phases near $x \approx 0.50$ at room temperature. Conventionally, these excellent properties were attributed to the coexistence of T and R ferroelectric phases.

The PZT phase diagram of Ref. 1 was widely accepted until 1999, when Noheda *et al.*[2–4] reported a monoclinic phase in $Pb(Zr_{0.52}Ti_{0.48})O_3$ ceramics using high-energy x-ray diffraction. A phase transformational sequence of cubic(C) $\rightarrow$tetragonal(T) ferroelectric$\rightarrow$monoclinic ferroelectric was found. At the $T \rightarrow M$ transition, the lattice constant c remained essentially unchanged, while that of a_T split into a_m and b_m with a monoclinic angle of β-90° $\approx$0.5°. Mesh scans then revealed signatures of the monoclinic C (M_c) phase belonging to the space group Pm. The M_c unit cell is primitive having a unique b_m axis that is oriented along the pseudocubic [010], where the polarization is constrained to the (010) plane. Subsequently, the excellent piezoelectric properties of MPB ferroelectric crystals and ceramics have been attributed to M phases,[5–8] where the polarization is allowed to rotate in the monoclinic plane.

Pertsev *et al.*[9] calculated the epitaxial phase diagram for PZT thin layers using thermodynamics, as functions of x, temperature, and misfit strain. They predicted a M ferroelectric phase in MPB compositions of PZT films, which should also have superior dielectric and piezoelectric coefficients. However, experimentally, a monoclinic phase in PZT thin films has never been found. Foster *et al.*[10] grew single-crystal $Pb(Zr_{1-x}Ti_x)O_3$ films (1.0–2.5 μm) for $0<x<1$ on (001) $SrRuO_3/SrTiO_3$ by metal-organic chemical vapor deposition. They reported that the phase stability changed from orthorhombic (O)$\rightarrow R \rightarrow T$ with increasing Ti for $0.06<x<0.46$. In addition, PZT thin films with thickness of 1.5–2.0 μm have been deposited on differently oriented—(001), (110), and (111)—$SrRuO_3/SrTiO_3$ substrates.[11] For $0.25<x<0.8$, investigations have shown that T and R phases coexist over a wide compositional range about the MPB. The width of this two-phase field in compositional space depended on orientation and presumably epitaxial mismatch. It is noteworthy that thin films of other perovskite ferroelectrics—such as $BiFeO_3$—have been shown to have monoclinic phases that also have excellent ferroelectric properties.[12–14] For example, $BiFeO_3$ thin films have 20 times larger polarization than bulk $BiFeO_3$ crystals that have a stable R phase.

Here, we report the finding of a low symmetry M_c phase in $Pb(Zr_{0.52}Ti_{0.48})O_3$ epitaxial thin layers grown on (101) $SrRuO_3/SrTiO_3$ by pulsed laser deposition: corresponding films grown on (001) and (111) $SrRuO_3/SrTiO_3$ have T and R structures, respectively. We then show that the ferroelectric properties are superior in the M_c phase field of PZT.

First, a 50 nm layer of $SrRuO_3$ was grown by pulsed laser deposition (PLD) on top of (001), (101), and (111) $SrTiO_3$ substrates that had been ultrasonically cleaned. These layers were grown as bottom electrodes. Then, $Pb(Zr_{0.52}Ti_{0.48})O_3$ thin films were heteroepitaxially grown by PLD on top of $SrRuO_3/SrTiO_3$ with thicknesses between 50 and 200 nm. Films were deposited using a KrF laser (wavelength of 248 nm) by a Lambda 305i, focused to a spot size of 10 mm and incident on the surface of a target, using energy densities of 1.1 and 1.2 J/cm^2 for $SrRuO_3$ and PZT, respectively. The distance between the substrate and target was 6 cm; the base vacuum of the chamber was $<10^{-5}$ Torr. During film deposition, the oxygen pressure was 150 mTorr for $SrRuO_3$ and 60 mTorr for PZT. The growth rates of $SrRuO_3$ and PZT were 1 and 3 nm/min, respectively. After deposition, a number of gold electrode pads were deposited (through a mesh) on top of the PZT film by sputtering.

The crystal structure of the films was measured using a Philips X'pert high resolution x-ray diffractometer equipped with a two bounce hybrid monochromator, an open three-circle Eulerian cradle, and a domed hot stage. The analyzer was a Ge (220) cut crystal which had a θ resolution of 0.0068°. The x-ray unit was operated at 45 kV and 40 mA with wavelength of 1.5406 Å (Cu $K\alpha$). The reciprocal lattice unit corresponds to $a^* = 2\pi/a = 1.872$ Å^{-1}: the mesh scans presented in this letter are all plotted in this reciprocal unit. The resistivity and ferroelectric polarization of the films were

[a]Electronic mail: yan@vt.edu

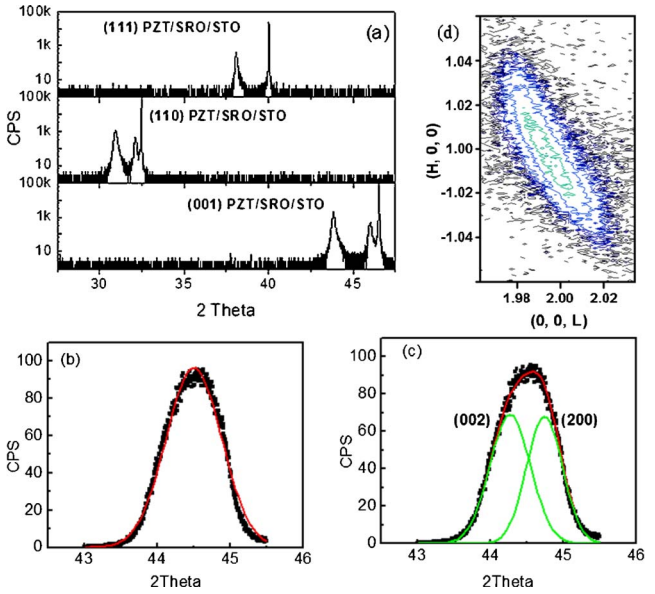

FIG. 1. (a) X-ray line scans over a wide 2θ range for (001), (101), and (111) oriented PZT films grown on $SrRuO_3/SrTiO_3$, demonstrating that the films are single crystalline and epitaxial; (b) line scans taken about the (002) and (200) peaks of a (101) oriented PZT thin film, fitted to a single Gaussian; (c) line scans taken about the (002) and (200) peaks of a (101) oriented PZT thin film, fitted to two Gaussians; and (d) (102) mesh scan.

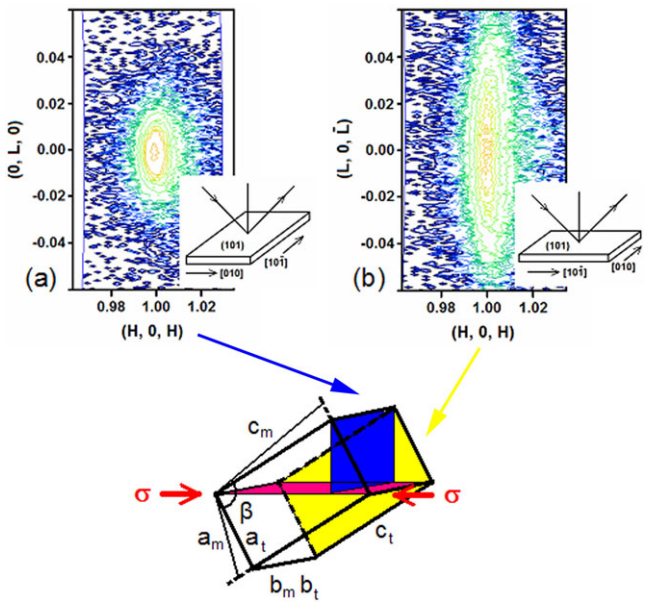

FIG. 2. Mesh scans taken about the (101) peak of a (101) oriented PZT thin film: (a) scattering plan is $(10\bar{1})$ and (b) scattering plan is (010). (c) Illustration of geometry of zones with respect to monoclinic distortion and orientation of in-plane compressive stress. The plane of the film is shown in pink, the $(10\bar{1})$ plane in blue, and the (010) plane in yellow.

then measured using a Radiant Technology workstation and Signatone probe station.

Figure 1(a) shows x-ray diffraction line scans taken over a wide 2θ range for (001), (101), and (111) oriented PZT films grown on $SrRuO_3/SrTiO_3$. The films were all epitaxial single crystals, well crystallized as evidenced by the sharpness of the peaks [$FWHM_{(002)} \approx FWHM_{(111)} \approx 0.06° - 0.08°$ and $FWHM_{(101)} \approx 0.12°$, where FWHM denotes full width at half maximum] and each 200 nm thick. Analysis then revealed that the lattice structure of (001) PZT film was tetragonal, as previously reported.[10,11] The lattice parameter c_t was determined to be 4.132 Å from the (002) scan and a_t to be 4.044 Å from the (002) and (101) ones. We next determined that the structure of (111) PZT films was rhombohedral, again as previously reported.[10,11] The lattice parameters were determined to be $a_r = 4.017$ Å and $90° - \alpha_r = 0.42°$ by analysis of (002) and (111) peaks.

Consistent with prior studies, no evidence of a monoclinic splitting was found in either (001) or (111) PZT films. However, we found the (101) oriented PZT film to be monoclinic. Figure 1 also shows line scans of {200} peaks of a 200 nm thick (101) film which were fitted by (b) a single Gaussian and (c) two Gaussians. Analysis revealed notably better fittings of the peak to two Gaussians, reflecting the fact that the (101) peak was wider than the others. The corresponding lattice parameters are $(c,a) = (4.098\ \text{Å}, 4.059\ \text{Å})$. Figure 1(d) is a (102) mesh scan, which is equivalent to (100)+(002). This figure illustrates an elongation along the $(H0\ L)$ direction, which consists of two $d_{(002)}$ values that are also tilted along the transverse direction with respect to each other. Although the film is thin and accordingly the two peaks are not clearly split, two Gaussians were needed to fit the peak. A third lattice parameter b was then determined from the (111) and (101) peaks to be 4.049 Å; in addition, an angle between the a and c axes of $\beta_m = 90.44°$ was calculated from $d_{(001)}$, $d_{(100)}$, and $d_{(101)}$ interatomic spacings. This structure is monoclinic with $(a_m, b_m, c_m; \beta_m) = (4.059\ \text{Å}, 4.049\ \text{Å}, 4.098\ \text{Å}; 90.44°)$. The fact that $\beta_m > 90°$ shows that this monoclinic phase is of the c type. In this case, the polarization is constrained to the (010) plane. Furthermore, since the (111) peak could not be fitted by two or three Gaussians and that $d_{(111)} = d_{(1\bar{1}1)}$, we can eliminate the possibility that the (101) PZT film is M_a or M_b.

The lattice mismatch (ϵ) between substrate and film was then calculated as $\varepsilon = [(a_{\text{film}} - a_{\text{substrate}})/a_{\text{substrate}}] \times 100\%$. Along $\langle 010 \rangle$, $b_m = 4.0485$ Å, $a_{\text{SRO}} = 3.950$ Å, and thus $\varepsilon = 2.49\%$, whereas along $\langle 10\bar{1} \rangle$, $d_{(10\bar{1})} = 2.873$ Å, $d_{(10\bar{1})\text{SRO}} = 2.793$ Å, and thus $\varepsilon_{(10\bar{1})} = 2.85\%$. This demonstrates that the constraint imposed on (101) films by the substrate are larger along $\langle 101 \rangle$ than $\langle 010 \rangle$. In Fig. 2, we show mesh scans taken perpendicular to the plane of (101) oriented PZT thin films by scanning along different directions: (a) scattering plane is $(10\bar{1})$ and (b) scattering plan is (010). The results clearly show that the transverse linewidth measured in (010) is much larger when the mesh scan is measured in $(10\bar{1})$. This confirms that the film is mainly stressed (compressive) in the $\langle 101 \rangle$ direction, which is required to stave the M_c phase. Figure 2(c) then illustrates the effect of the said constraint of PZT films grown on (101) $SrRuO_3/SrTiO_3$ substrates. The difference between the b lattice parameters of the M and T phases is $(a_t - b_m) = 0.005$ Å, whereas that of the c is $(c_t - c_m) = 0.035$ Å. Thus, for (101) films relative to (001), the compressive stress along $\langle 10\bar{1} \rangle$ forces c_m to be shorter than c_t, enlarging β to $>90°$ instead and then make c_m rotate along the $\langle 010 \rangle$ direction as shown in Fig. 2(c); furthermore, since the compressive stresses are nearly equal along $\langle 010 \rangle$, $b_m \approx a_t$.

The conceptual reason for the formation of the M_c phase in (101) oriented PZT thin films is similar to that for field-cooled (FC) $Pb(Mg_{1/3}Nb_{2/3})O_3 - (x\ \text{at.}\ \%)PbTiO_3$ (PMN–x%PT) single crystals, where the structure can be

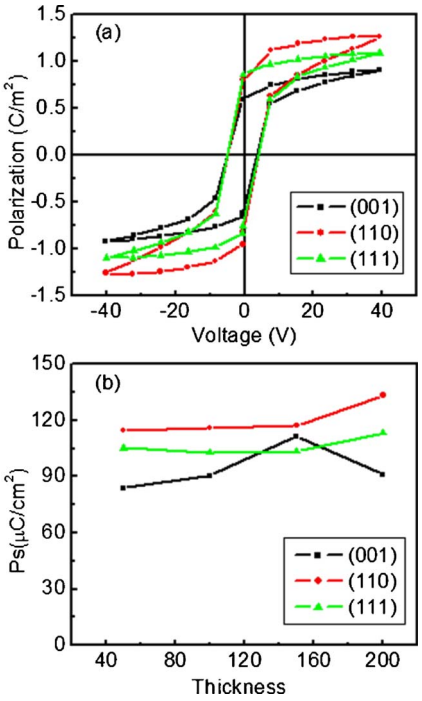

FIG. 3. Polarization of variously oriented PZT thin films: (a) dependence of polarization on electric field (*P-E*) and (b) dependence of saturation polarization of film thickness.

changed from cubic to M_b or M_c in the FC condition by application of electric field (E) along [110] (Ref. 15) or [001],[16] respectively. In general, the effect of epitaxy is similar to that of $E//[001]$—it fixes the direction of the c axis to be close to that of an ordering force. In this M_c phase, the polarization lies in the (001) plane and rotates towards [100] with (a) increasing E for PMN–x%PT and (b) presumably with increasing epitaxial stress for (101) PZT layers.

We next measured the ferroelectric properties of our PZT films. First, we confirmed that all of the films were highly insulating, having resistivities of $\rho \geqslant 10^{10} \sim 10^{11}\Omega$ cm, which is sufficient to perform high field polarization studies. In Fig. 3(a), we show the polarization electric field (i.e., *P-E*) response of (001), (101), and (111) oriented films. These data were taken using a measurement frequency of 10 kHz on 200 nm thick films. The data show that the saturation polarization P_s is highest for the (101) oriented film: $P_s(001)=0.9\ \mathrm{C/m^2}$, $P_s(111)=1.1\ \mathrm{C/m^2}$, and $P_s(101)=1.3\ \mathrm{C/m^2}$. These results confirm that (i) the monoclinic C phase of MPB PZT epitaxial films has the highest polarization and (ii) for (110) epitaxial film, the polarization lies in the (0H0) plane between the [101] and [001] directions. We then show in Fig. 3(b) that the value of P_s for the variously oriented films is nearly independent of film thickness for $50 < t < 20$ nm.

In summary, we show that structure of $Pb(Zr_{0.52}Ti_{0.48})O_3$ is dependent upon the orientation of the $SrRuO_3/SrTiO_3$ substrate on which it is deposited: T for (001), R for (111), and M_c for (101). This is the report of a monoclinic phase in PZT epitaxial thin layers: it is stabilized by a compressive stress directed along $\langle 10\bar{1} \rangle$. We then demonstrate that the polarization is the highest when M_c is the stable phase.

The authors would like to gratefully acknowledge financial support from the U.S. Department of Energy under Contract No. DE.-AC02-98CH10886, Office of the Air Force Office of Scientific Research under FA 9550-06-1-0410, and the Office of Naval Research under Grant No. N00014-06-1-0204.

[1] B. Jaffe, W. R. Cook, and H. Jaffe, *Piezoelectric Ceramics* (Academic, New York, 1971), p. 136.
[2] B. Noheda, D. E. Cox, G. Shirane, J. A. Gonzalo, L. E. Cross, and S. E. Park, Appl. Phys. Lett. **74**, 2059 (1999).
[3] B. Noheda, J. A. Gonzalo, L. E. Cross, R. Guo, S. E. Park, D. E. Cox, and G. Shirane, Phys. Rev. B **61**, 8687 (2000).
[4] B. Noheda, D. E. Cox, G. Shirane, R. Guo, B. Jones, and L. E. Cross, Phys. Rev. B **63**, 014103 (2000).
[5] H. Fu and R. E. Cohen, Nature (London) **403**, 281 (2000).
[6] B. Noheda, D. E. Cox, G. Shirane, S. E. Park, L. E. Cross, and Z. Zhong, Phys. Rev. Lett. **86**, 3891 (2001).
[7] J. M. Kiat, Y. Uesu, B. Dkhil, M. Matsuda, C. Malibert, and G. Calvarin, Phys. Rev. B **65**, 064106 (2002).
[8] H. Cao, J. Li, D. Viehland, and Guangyong Xu, Phys. Rev. B **73**, 184110 (2006).
[9] N. A. Pertsev, V. G. Kukhar, H. Kohlstedt, and R. Waser, Phys. Rev. B **67**, 054107 (2003).
[10] C. M. Foster, G. R. Bai, R. Csencsits, J. Vetrone, R. Jammy, L. A. Wills, E. Carr, and Jun Amano, J. Appl. Phys. **81**, 2349 (1997).
[11] S. Yokoyama, Y. Honda, H. Morioka, S. Okamoto, H. Funakubo, T. Iijima, H. Matsuda, K. Saito, T. Yamamoto, H. Okino, O. Sakata, and S. Kimura, J. Appl. Phys. **98**, 094106 (2005).
[12] J. Wang, J. B. Neaton, H. Zheng, V. Nagarajan, S. B. Ogale, B. Liu, D. Viehland, V. Vaithyanathan, D. G. Schlom, U. V. Waghmare, N. A. Spaldin, K. M. Rabe, M. Wuttig, and R. Ramesh, Science **299**, 1719 (2003).
[13] J. Li, J. Wang, M. Wuttig, R. Ramesh, N. Wang, B. Ruette, A. P. Pyatakov, A. K. Zvezdin, and D. Viehland, Appl. Phys. Lett. **25**, 5261 (2004).
[14] G. Xu, H. Hiraka, G. Shirane, J. Li, J. Wang, and D. Viehland, Appl. Phys. Lett. **86**, 182905 (2005).
[15] H. Cao, F. Bai, N. Wang, J. Li, D. Viehland, G. Xu, and G. Shirane, Phys. Rev. B **72**, 064104 (2005).
[16] H. Cao, J. Li, D. Viehland, G. Xu, and G. Shirane, Appl. Phys. Lett. **88**, 072915 (2006).